Atomistic Modelling of III-V Semiconductors: from a single tetrahedron to millions of atoms

M.A. Migliorato [a*], V. Haxha[a], R. Garg[a], I.W. Drouzas[b], J. M. Ulloa[c], P. M. Koenraad[c], M. J. Steer[d], H. Y. Liu[e], M. Hopkinson[f], D. J. Mowbray[b]

[a] *School of Electrical and Electronic Engineering, University of Manchester, UK.*
[b] *Department of Physics and Astronomy, University of Sheffield, UK.*
[c] *Photonics and Semiconductor Nanophysics, Technical University Eindhoven, NL.*
[d] *Electronics and Electrical Engineering, University of Glasgow UK.*
[e] *Department of Electronic and Electrical Engineering, University College London, UK.*
[f] *Department of Electronic and Electrical Engineering, University of Sheffield, UK.*

* Corresponding author: max.migliorato@manchester.ac.uk

Abstract

Modelling of III-V semiconductor materials and nanostructures has been a very active field in the last 15 years. The rapid development in the material synthesis of low dimensional structures for optical applications has triggered a world wide interest for modelling methods capable of accurately describing systems comprising millions of atoms. With the development of empirical or semiempirical methods, together with the ever increasing computational power available to scientists, it is now possible to model e.g. quantum dots inside simulation boxes comprising 3 million atoms.

In this talk we will review the most recent developments in the field of empirical atomistic methods, particularly the bond order potentials, and discuss its links and reliance on ab initio calculations. The links between these methods and modeling of segregation effect will also be discussed.

1. INTRODUCTION

Atomistic empirical potential methods [1], [2], [3] for molecular dynamics (MD) and molecular statics (MS) are now very often used in structural simulations of low dimensional semiconductors [4]. The modelling work is driven by the need to model the electronic properties of epitaxially grown semiconductors, particularly when lattice mismatch is present. The electronic properties are in fact strongly related to the structural properties of the crystals and hence the accurate determination of elastic and strain properties has become an essential step.

Furthermore because of computational efficiency these techniques become the only method possible for semiconductor crystals lacking long ranged symmetry, e.g. the cases of defects inclusions [5], compositional disorder in complex ternary alloys and nanostructures [5],[6]. Recently [7], [8], [9] much experimental work on quaternary alloys such as InGaAsN or InGaAsSb has taken place and questions on the nature of the elastic properties of the binary compounds and how these are related to those of the quaternary alloys have become a fundamental question. A question that empirical emprirical potentials can solve since the simulation cell size is not restricted like in the case of ab initio calculations.

2. THE TERSOFF POTENTIAL

This emprirical potential [1] was formulised to mimic the exponential Morse-like pair bonding but at the same time introduce a many-body term to account for local neighbours (both in terms of the distance from the atom under consideration and the subtended bonding angle). This represents a substantial improvement compared to other empirical potentials such as the Stillinger-Weber potential [2],[3], because of the better description of the chemistry of the bonds, and also the Keating-Valence Force Field [2]method, because of the possibility of treating non-tetrahedral systems and the ability to provide a better description of the anharmonic region of the energy vs. bond length curve. The original form of is shown below with a couple of modifications to nomenclature for compatibility with other authors:

$$E = \frac{1}{2}\sum_{j\neq i} f_c(r_{ij})\left(V_R(r_{ij}) - b_{ij}V_A(r_{ij})\right) \tag{1}$$

The pairwise terms V_A and V_R are classical pairwise attractive and repulsive terms, whereas b_{ij} is a many body term that scales the attractive part to the repulsive one, the functional form of which will be given later. The pairwise terms are written as:

$$V_R = \frac{D_e}{S-1}\mathrm{e}^{-\beta\sqrt{2S}(r_{ij}-r_e)} \tag{2}$$

$$V_A = \frac{SD_e}{S-1}\mathrm{e}^{-\beta\sqrt{2/S}(r_{ij}-r_e)} \tag{3}$$

These last expressions use different parameters (D_e, S, β, r_e) from the ones used in the original paper by Tersoff [1], but are identical in substance. To restrict the calculation to just a certain number of nearest neighbours of the atom *i* under

observation, a spherical cut off function f_c is introduced:

$$f_c(r) = \begin{cases} 1 & r_{ij} < R - R_{cut} \\ \frac{1}{2}\left[1 - \sin\left[\pi(r_{ij} - R)/2R_{cut}\right]\right] & \left|r_{ij} - R\right| \le R_{cut} \\ 0 & r_{ij} > R + R_{cut} \end{cases} \quad (4)$$

so that the parameters R and R_{cut} determine the position of the cut off and the half width of the region in which the function changes smoothly from 0 to 1.
The many body term b_{ij}, which depends on the parameters γ and n, can be expressed as:

$$b_{ij} = \left[1 + \left(\gamma\zeta_{ij}\right)^n\right]^{-1/2n} \quad (5)$$

which is intentionally designed to have a -1/2 power dependence in respect of the number ζ_{ij}. In fact ζ_{ij} provides a weighted measure of the number of other bonds, labeled k, competing with the bond ij and models the coordination number Z of the open-lattice semiconductor material. The pseudo coordination number ζ_{ij} is a function of the local environment. In fact it is expressed in terms of the cut off function f_c, a function $g(\theta)$ which takes in account the angular dependence, an exponential function ω_{ijk} that tunes the radial dependence and a set of atom type dependent parameters (γ, n, c, d, h, λ):

$$\zeta_{ij} = \sum_{k \neq i,j} f_c(r_{ik}) \cdot g(\theta_{ijk}) \cdot \omega_{ijk} \quad (6)$$

where $g(\theta)$ is expressed by:

$$g(\theta_{ijk}) = 1 + \left(\frac{c}{d}\right)^2 - \frac{c^2}{d^2 + (h - \cos\theta_{jki})^2} \quad (7)$$

with θ_{ijk} the angle between bonds ij and ik. It has been demonstrated that the choice of functional form is not arbitrary, as the mathematical expression of the angular function $g(\theta)$ is equivalent to that obtained as a Tight Binding expansion of the electronic density of states to its second moment.[10]
The role of the exponential factor in the expression for ζ_{ij} is to reduce the otherwise unrealistic influence of distant neighbours on immediate bonds. [11]

$$\omega_{ijk} = \exp\left[\lambda^3 (r_{ij} - r_{ik})^3\right] \quad (8)$$

The evaluation of the materials properties chosen to parameterise the potential follows standard procedures. The equilibrium lattice constant a and cohesive energy E_{coh} are easily estimated from the energy vs bond length relationship at the energy minimum. Evaluation of the Bulk Modulus and shear constant C' is obtained through an hydrostatic and a non-uniform deformation. These quantities can be directly related in the zinc blende crystals to the elastic constants c_{11} and c_{12}. The third elastic constant, c_{44} is related to shear deformation in the plane.
however when performing this calculation one has to take into account the internal displacements which move the interpenetrating *fcc* sublattices in the diamond structure along the z axis, and therefore minimise the energy for every given γ, with respect to this internal displacement. The condition of minimum energy is characterised by the Kleinman's internal displacement parameter ζ,[12] which defines the displacement as being $\zeta\gamma a/4$, with a being the lattice constant.
This parameter has a deep meaning. If one concentrates on a single tetrahedron with e.g a cation in the origin of the coordinate system, a positive shear distortion tends to pull apart two cations along the [110] direction, while pulling together the other two cations in the [1$\bar{1}$0] direction. Because of these movements the anion at the centre of the tetrahedron is subject to radial and angular forces, which resist bond length and bond angles change respectively, and the displacement that minimises the total energy is a result of a subtle balance between the two.[4] Hence correctly reproducing this effect is an indication that the angular and radial functions in the functional form of the potential are correctly balanced.

3. ATOMISTIC MODELS OF ALLOYS

In order to obtain the numerical values that are needed for the parameterizations we can often rely on experimental values, but for e.g. the Kleinmann deformation only some values are available from ab initio calculations. We have therefore also implemented some Density Functional calculations in the local density approximation to obtain the missing data. Since these calculations are often done on a single dimer, with periodic cells, we can say that overall we study semiconductors from a single tetrahedron up to the millions of atoms that empirical potentials allow. The parameterizations obtained for InAs, GaAs, InSb and GaSb with the method previously explained have already been reported [4]. This parameterization are particularly

suited to model pseudomorphically strained semiconductors and their alloys, in the linear regime but also well reproduces the linear and higher order effects of sublattice displacement under shear strain. In disordered alloys these effects can be large even in pseudomorphic layers.

To study the strain properties of the $In_xGa_{1-x}Sb_yAs_{1-y}$ alloy pseudomorphically grown on GaAs [001] substrates as a function of *x* and *y* we built a series of 100 atomistic models of $In_xGa_{1-x}Sb_yAs_{1-y}$ /GaAs Quantum Wells with different composition. In each simulation we systematically varied the relative fractions *x* and *y* of group III and group V elements. Care has been taken to ensure the general validity of the predictions and independence of the results from particular atomic arrangements. For example we chose the size of the simulation box as to minimize fluctuations in the elastic energy due to compositional disorder. The structures are relaxed (molecular statics implementation) using a parallel implementation of the IMD™ software [13]. From the relaxed atomic positions we evaluated the crystal strain energy by taking the local composition under consideration and by evaluating the strain on each tetrahedron in the crystal. From the local strain components we can easily obtain the average elastic potential energy, which unlike the strain tensor is a non local property and hence it is better suited to describe the elastic properties of a disordered alloy.

In this work we also present an improved model for segregation in quaternary alloys in order to introduce a correlation between group III and V exchanges.

4. SEGREGATION IN QUATERNARY ALLOYS

Surface segregation is the physical effect which is known to occur during the epitaxial growth of GaInAs or GaAsSb alloys by MBE [14],[15], resulting in one or more atomic species not being incorporated in the crystal and instead segregate on the growing surfaces [16],[17],[18][19].

In the classic kinetic model of segregation [20] the exchange processes of either cations or anions are treated separately in terms of mass conservation equations and kinetic processes that are regulated by Arrhenius style exponential functions of the hopping or exchange energies. However in quaternary alloys the coupling of the anion and cation exchange is essential and we implement this by altering the exchange energies of the atoms in different layers and making it a function of the elastic strain energy. In this way for the case of e.g InGaAsSb the In/Ga exchange process depends on the amount of Sb and the Sb/As exchange process depends on the amount of In present.

In the classic kinetic model segregation is an exchange process and the evolution of the number of In surface atoms is given by the balance of incoming and leaving In or Ga atoms [20].

$$\frac{dX_{In->s}(t)}{dt} = \phi_{In} + P_1 * X_{In->b}(t) * X_{Ga->s}(t) - P_2 * X_{In->s}(t) * X_{Ga->b}(t) \tag{9}$$

Where ϕ is the impinging flux in ML/s and the $X_i(t)$ are the time dependent concentrations expressed in fraction of monolayer. At the time interval *dt*, the number of In atoms approaching in the surface layer is the sum of the impinging In flux and P_1 rate weighted by the number of exchange possibilities which is taken as the product $X_{In->b}(t)\ X_{Ga->s}(t)$, The reverse exchange results in a number of In atoms leaving the surface phase given by $P_2\ X_{In->s}(t)\ X_{Ga->b}(t)$.The total surface atom numbers at time *t* can be written by the expression:

$$X_{In->s}(t) + X_{In->b}(t) = X_{In->s}(0) + X_{In->b}(0) + \phi_{In} * t \tag{10}$$

$$X_{In->s}(t) + X_{Ga->s}(t) = X_{In->s}(0) + X_{Ga->s}(0) + (\phi_{In} + \phi_{Ga}) * t \tag{11}$$

The probabilities of exchange are described by:

$$P_1 = \nu_1 e^{-\frac{E_1}{kT}}$$

$$P_2 = \nu_2 e^{-\frac{E_2}{kT}} \tag{12}$$

(13)

where the $\upsilon_1 = \upsilon_2 = 10^{13}\ s^{-1}$ values [20],[18] are the vibration frequencies, and they are the combination of surface and bulk lattice vibration frequencies. Equations 10 to 13 can be easily written for Sb/As exchange by replacing In with Sb and Ga with As.

The two exchange energies for cation (Ga/In) are taken as the value proposed from [20] , $E_1 = 1.8$ eV and $E_2 = 2.0$ eV, and the exchange energies for anion (Sb/As) are taken from [18] , $E_1 = 1.68$ eV and $E_2 = 1.75$ eV.

These equations can be solved using the *Runge-Kutta* method [21] once they are combined to obtain an equation for $X_{In\ ->s}(t)$ or $X_{Sb->s}(t)$. The In or Sb concentration profile is then build from the numerical solution.

In our modification the exchange energies becomes:

$$P_1 = \nu_1 e^{-\left(\frac{E_1}{kT} + \frac{E_{SE}}{kT}\right)} \tag{14}$$

$$P_2 = \nu_2 e^{-\left(\frac{E_2}{kT} - \frac{E_{SE}}{kT}\right)}$$

(15)

Where the E_{SE} for e.g. the Sb/As segregation we define as the difference in elastic strain energy between a layer of InGaAsSb and one of GaAsSb:

$$E_{SE} = E_{StrainEnergy}\left(X_{In\to S}(t), \phi_{Sb}\right) - E_{StrainEnergy}\left(0.0, \phi_{Sb}\right) \tag{16}$$

For the In/Ga exchange a similar expression is also appropriate.

5. RESULTS OF THE SIMULATIONS

The average elastic strain energy per atomic structure of a sufficiently thick epitaxial layer of the $In_xGa_{1-x}Sb_yAs_{1-y}$ alloy for all combinations of the atomic fractions *x* and *y* is shown in inset of Fig. 2. It shows that the strain energy does not follow simple linear averages. In fact the maxima is obtained when both In and Ga are present together with Sb. This is in large part an effect due to compositional disorder as we also tested equivalent superlattice structures with alternating InAs and GaSb layers and in that case the elastic energy is found to be lower. We can also conclude that the quaternary alloy is a metastable configuration and decomposition into ternary alloys is an energy favorable process.

Such predicted behaviour is confirmed experimentally. Self assembled quantum dots (QDs) are now routinely capped with a strain reducing layer (SRL) in order to achieve emission energy in the region of the electromagnetic spectrum suitable for

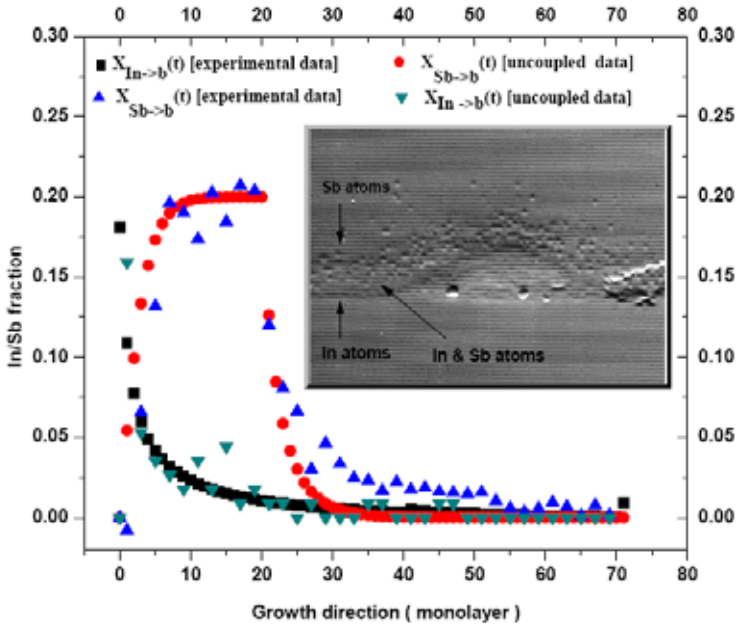

Fig. 1: The uncoupled In / Sb concentration profile, compared with experimental data. The In and Sb segregation during the growth of GaSbAs on InGaAs (inset image).

applications in the telecommunication range 1.3-1.55μm [22],[23],[24],[25]. In the inset of Fig. 1 we show a Scanning Tunnelling Microscopy (STM) image of an MBE InAs QD grown with a GaAsSb SRL. The details of the sample are as follows: a GaAs [001] substrate was covered by a GaAs buffer, followed by a 2.5 ML InAs layer, 6 nm GaSbAs and were finally capped with 100 nm GaAs. When GaAs is used as a capping material strong intermixing [26].

This is clearly in agreement with the results of our calculations which indicate that the quaternary alloy has a maximum in the energy landscape and is hence an unstable point. Phase separation into ternary or binary compounds is a much more likely event.

Chemical analysis of the In and Sb fraction from the STM data is presented in Fig. 1 together with the predicted profiles obtained using the classic uncoupled model of segregation. From the image it is clearly evident that the Sb exchange does not mach with experimental data. In fact the Sb concentration is experimentally found to raise and decay more slowly than what the model predicts.

When we use our coupled model with the exchange energies modified using the elastic energy data, our data (Fig. 2) shows a much improved agreement with experimental data.

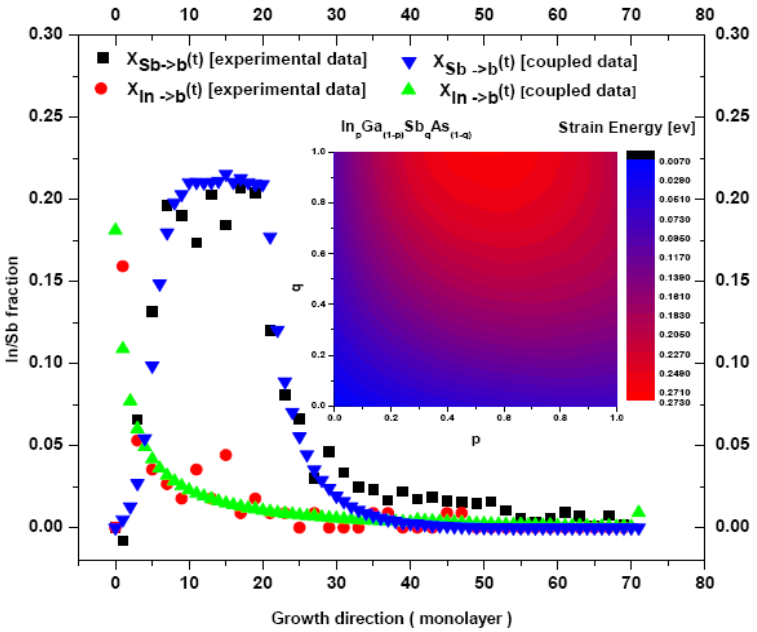

Fig. 2: The coupled In/Sb concentration profile, compared with experimental data, and the average elastic strain energy (inset image).

The difference between the uncoupled and coupled method is substantial. It is worth stressing that in the coupled method we do not use the exchange energies as fitting parameters. We simply modify the exchange energies of the uncoupled method using our knowledge of the strain energy.

The coupled model of segregation for the Sb profile differs from the uncoupled model in the raise and decay of the concentration which are in both case slower and in better agreement with experimental data. Furthermore in the uncoupled model the highest value of the concentration profile can never be higher than the value of the nominal flux. In the coupled method this is no longer true and accumulation is possible, though mass conservation is still maintained.

In conclusion we also show the strain maps obtained form a complete atomistic simulation of the quantum dot and SRL of the inset of figure 1. Such simulation comprises 3 million atoms.

7. REFERENCES

[1] J. Tersoff, Phys. Rev. Lett. 56, 632 (1986); Phys. Rev.B 37, 6991 (1988); Phys. Rev. B 39, 5566 (1989)

[2] P. N. Keating, Phys. Rev. 145, 637 (1966); 149, 674 (1966).

[3] F. H. Stillinger, T. A. Weber, Phys. Rev. B 31, 5262 (1985).

[4] D. Powell, M. A. Migliorato, and A. G. Cullis, Phys. Rev. B 75, 115202 (2007).

[5] T. Hammerschmidt, P. Kratzer, and M. Scheffler, Phys. Rev.B 75, 235328 (2007).

[6] M.A. Migliorato, D. Powell, S.L. Liew, A.G. Cullis, M. Fearn and J.H. Jefferson, P. Navaretti, M.J. Steer, M. Hopkinson, J. Appl. Phys. 96, 5169 (2004)

[7] N. Kouklin, H. Chik, J. Liang, M. Tzolov, J.M. Xu, J.B. Heroux,W.I. Wang, J. Phys. D: Appl. Phys. 36 2634 (2003).

[8] V.M. Ustinov, A. Y. Egorov, V. A. Odnoblyudov, N. V. Kryzhanovskaya, Y. G. Musikhin, A. F. Tsatsul'nikov and Z. I. Alferov, J. Cryst. Growth 251, 388 (2003).

[9] B.R. Bennett, B.V. Shanabrook, E.R. Glaser, R. Magno, M.E. Twigg, Superlattices Microstruct. 21, 267 (1997).

[10] D. Conrad and K. Scheerschmidt, Phys. Rev. B 58, 4538 (1998).

[11] M. Sayed, J. H. Jefferson, A. B. Walker, and A. G. Cullis, Nucl. Instrum. Methods Phys. Res. B 102, 218 (1995).

[12] L. Kleinman, Phys. Rev. 128, 2614 (1962).

[13] J. Stadler, R. Mikulla, and H.-R. Trebin, Int. J. Mod. Phys. C 8, 1131(1997).

[14] J. Nagel, J.P. Landesman, M. Larive, C. Mottet, P. Bois, J. Cryst. Growth 127, 550 (1993).

[15] K. Muraki, S. Fukatsu, Y. Shiraki, Appl. Phys. Lett. 61, 3 (1992).

[16] K.Yamaguchi, T. Okada, F. Hiwatashi, Appl. Surf. Sci. 117/118, 700 (1997).

[17] S.Y. Karpov, Y. N. Makarov, Thin Solid Films. 380, 71 (2000).

[18] R. Magri, A. Zunger, Phys. Rev. B 64, 081305 (2001).

[19] Y. N. Drozdov, N. V. Baidus, B. N. Zvonkov, M. N. Drozdov, O. I. Khrykin, V. I. Shashkin, Semiconductors. 37, 2 (2003)

[20] O. Dehaese, X. Wallart, and F. Mollot, Appl. Phys. Lett. 66, 52 (1995).

[21] W. H. Press, S. A. Teukolsky, W. T. Vetterling, B. P. Flannery, Numerical Recipes in C++, Cambridge University Press, New York (2002).
[22] H.Y. Liu, Y. Qiu, C.Y. Jin, T. Walther, A.G. Cullis, Appl. Phys. Lett 92, 111906 (2008).
[23] H.Y. Liu, M.J. Steer, T.J. Badcock, D.J. Mowbray, M.S. Skolnick, P. Navaretti, K.M.Groom, M. Hopkinson, R.A. Hogg, Appl. Phys. Lett. 86, 143108 (2005).
[24] H.Y. Liu, M.J. Steer, T.J. Badcock, D.J. Mowbray, M.S. Skolnick, F. Suarez J. S. Ng, M. Hopkinson, J.P.R. David, J. Appl. Phys. 99, 046104 (2006).
[25] J. Tatebayashi, M. Nishioka, Y. Arakawa, Appl. Phys. Lett. 78, 3469 (2001).
[26] Ch. Heyn, W. Hanse, J. Cryst. Growth. 251, 140 (2003) .